Site-Specific Pre-Swelling-Directed Morphing Structures of Patterned Hydrogels

Zhi Jian Wang, Wei Hong, Zi Liang Wu,* and Qiang Zheng

Abstract: *Morphing materials have promising applications in various fields, yet how to program the self-shaping process for specific configurations remains a challenge. Herein we show a versatile approach to control the buckling of individual domains and thus the outcome configurations of planar-patterned hydrogels. By photolithography, high-swelling disc gels were positioned in a non-swelling gel sheet; the swelling mismatch resulted in out-of-plain buckling of the disc gels. To locally control the buckling direction, masks with holes were used to guide site-specific swelling of the high-swelling gel under the holes, which built a transient through-thickness gradient and thus directed the buckling during the subsequent unmasked swelling process. Therefore, various configurations of an identical patterned hydrogel can be programmed by the pre-swelling step with different masks to encode the buckling directions of separate domains.*

Adaptive materials with morphing structures have received increasing attention owing to their promising applications in areas, such as biomedical devices, soft robotics, morphing aircrafts.[1–4] In this area, nature has provided excellent sources of inspiration.[5–8] For instance, pinecones and bean pods show smart deformations to release the seeds under desiccation.[5,6] These programmed deformations typically originate from the heterogeneous structures of plant organs, which build up internal stress under external stimuli. Inspired by these natural active systems, scientists have realized programmable deformations in artificial systems, such as bending, folding, and twisting, by creating through-thickness and/or in-plane gradient structures.[9–18] For example, controllable bending and folding are realized by incorporating

a gradient structure in the thickness direction of a slender material.[11,13] Under stimuli, the differential volume change and stress across the thickness lead to controllable deformations. In recent years, researchers found that in-plane heterogeneities can also lead to modulated internal stresses and thus three-dimensional (3D) deformations.[19–23] A seminal work by Sharon et al. showed that a disc-shaped hydrogel sheet with in-plane gradient deforms into a dome shape or develops edge wrinkles when the central part contracts less or more, respectively.[19] By using photolithography, more complex distributions of components and internal stresses can be encoded in the planar-patterned hydrogels, leading to various 3D configurations under external stimuli.[20–22] By combining such in-plane and through-thickness gradients in a hydrogel strip, twisting deformation was realized, similar to the spontaneous opening of seed pods.[15,24]

More complex configurations can be obtained by stacking individual structures of typical forms, each responsible for one mode of deformation in the integrated system, such as localized bending, folding, and twisting.[25–31] Specifically, the combination of bending and folding by creating through-thickness gradients has been intensively investigated to form elaborate configurations, enabling encapsulation or handling of objects.[26–29] Comparing to those with through-thickness gradients, in-plane gradient structures are stackable and can be easily integrated by photolithography for more complex patterns. However, in terms of the direction control, the in-plane gradient-induced buckling is less predictable than the through-thickness gradient-induced bending. Through-thickness gradient-induced bending has a well-defined direction, whereas in-plane gradient-induced buckling has an equal probability of buckling upward or downward because there is no gradient in the thickness direction.[19,23] Indeed, the in-plane gradient-induced buckling deformation is known to have self-locked bi-stable states,[32] and the composite patterned hydrogels with n buckling units will have 2^n configurations in total. The arbitrary buckling direction makes it difficult to controllably arrive at a specific metastable configuration on demand. To address this issue, we need to find a facile approach to locally control the buckling direction of the patterned hydrogel with in-plane gradients.

We demonstrate herein a versatile strategy to realize programmable deformations of patterned hydrogel sheets with series of dome-like structure as the building block that buckled into the desired direction with the assistance of a pre-swelling step. Using photolithography, an array of high-swelling gel discs was embedded in a non-swelling hydrogel. A pair of masks with holes were placed on both sides of the patterned hydrogel sheet to induce site-specific swelling after being immersed in water. The high-swelling gel regions under

[*] Z. J. Wang, Prof. Z. L. Wu, Prof. Q. Zheng
Key Laboratory of Macromolecular Synthesis and Functionalization of Ministry of Education
Department of Polymer Science and Engineering
Zhejiang University
Hangzhou 310027 (China)
E-mail: wuziliang@zju.edu.cn

Prof. W. Hong
Department of Aerospace Engineering, Iowa State University
Ames, IA 50010 (USA)
and
Department of Engineering Mechanics, Zhejiang University
Hangzhou 310027 (China)
and
Global Station for Soft Matter, Global Institution for Collaborative Research and Education, Hokkaido University
Sapporo 060-0810 (Japan)

⬚ Supporting information and the ORCID identification number(s) for
ⓘD the author(s) of this article can be found under:
https://doi.org/10.1002/anie.201708926.

the holes were selectively swollen, whereas other regions were masked, resulting in a built transient through-thickness gradient in specific regions. The transient through-thickness gradient induced bending deformation of the high-swelling gel, which was taken over by the in-plane gradient-induced buckling during the subsequent unmasked free-swelling process. Via this pre-swelling step, the buckling direction of each domain was controlled, leading to the formation of complex, yet programmed configuration of the patterned hydrogel. The deformed hydrogel can be flattened again after being swollen in saline solution to diminish the swelling mismatch between the high-swelling and non-swelling gels, and another round of procedure with the pre-swelling step can be applied to the identical hydrogel using different masks to direct the formation of distinct configurations. This work provides a straightforward approach to control the deformation of patterned hydrogel sheets into desired configurations, which should expand the applications of morphing materials in sensing and actuation.

Figure 1 shows the preparation of the patterned hydrogels and the concept of pre-swelling-directed deformation. The composite gel strip, in which an array of poly(acrylamide-co-2-acrylamido-2-methylpropanesulfonic acid) (P(AAm-co-AMPS)) gel discs were surrounded by polyacrylamide (PAAm) gel, was prepared by a two-step photo-polymerization (Figure 1 a–c; see details in Supporting Information). If

the as-prepared patterned hydrogel was freely swelled in water, the different swelling capacities and Young's moduli of P(AAm-co-AMPS) and PAAm gels (Figure S1a, in the Supporting Information) led to out-of-plane buckling of the high-swelling disc gel and the formation of dome-like shape.[19,23] The integrated patterned gel formed a roll (Figure 1 d), that is, the domes buckled in the same direction, as a result of the interaction of neighboring domains to minimize the total elastic energy. Other configurations were energetically unfavorable and suppressed during the free-swelling process. However, the deformation pathway can be altered by a site-specific pre-swelling step and thus to locally control the buckling direction ahead and during the free-swelling of the integrated hydrogel.[33,34] As shown in Figure 1 e–g, the neighboring domains buckled into opposite directions, and the patterned gel strip remained flat overall.

Without mask or perturbation, the high-swelling domains in a free-swelling sample always buckle in the same direction. To elucidate the mechanism, further experiment and numerical simulation (see details in the Supporting Information)[35,36] were performed on patterned gels with two basic units, and the energy profiles were compared between distinct buckled configurations (Figures 1 h,i). As expected, the buckled state of both domes on the same side (mode I) always possesses a lower total elastic energy than the one with domes in opposite directions (mode II; Figure 1 j). As shown by Figure 1 i, the major difference lies in the interconnecting region, where the seemingly flatter morphology in mode II causes higher in-plane stretches to accommodate the localized change in curvature. However, the two states separated by a relatively high energy barrier and thus are both mechanically stable. The free-swelling process selects mode I simply because the critical mismatch strain for mode I is lower. Transformation between the two modes requires external perturbations, for example, by applying a force to induce the snap of one unit. A more efficient strategy is to direct the buckling direction at the beginning of swelling process, when the energy barrier between is relatively low. By selectively swelling from one side of the hydrogel sheet, the transient through-thickness gradient of swelling ratio will bend the gel in the opposite direction.[33,34]

Owing to the significantly lower energy well in mode I, sufficient swelling time is needed to direct the gel away from the neutral state and develop sustainable amplitude for the desired buckling mode. A gel strip containing six high-swelling discs was used to investigate the influence of pre-swelling time and gel thickness on the selection of deformation modes (buckling into the same direction or alternatively into opposite directions; Figure 2 a). As shown in Figure 2 b–d, a critical pre-swelling time, t_c, was needed for mode II deformation. If the pre-swelling time, t, was insufficient ($t < t_c$), the preliminary deformation of mode II cannot maintain its configuration to equilibrium state; instead, it transformed to mode I during the subsequent free-swelling process (Figure 2 d and Figure S2). Furthermore, it was found that the critical pre-swelling time t_c scaled with the squared of the sample thickness T: $t_c \approx T^2$ (Figure 2 c), indicating that the mode selection is governed by the diffusion-induced through-thickness gradient of swelling ratio—as the water is diffusing
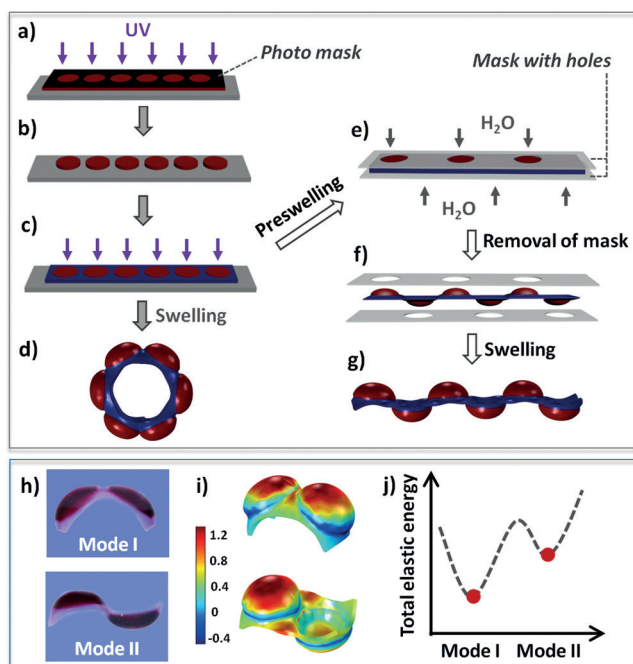

Figure 1. a)–g) Preparation of patterned hydrogels and the swelling-induced deformations. The composite gel strip was prepared by two-step photo-polymerization (a–c). Red: high-swelling gel; blue: non-swelling gel. The as-prepared composite gel strip formed a roll after free-swelling in water (d). In contrast, a programmable configuration can be obtained via a pre-swelling step to direct the buckling direction of localized domains (e–g). h)–j) Experimental (h) and computed (i) results of bi-stable configurations of patterned gel with two domes and their relative total elastic energy (j). The color scale in (i) indicates the in-plane areal strain.
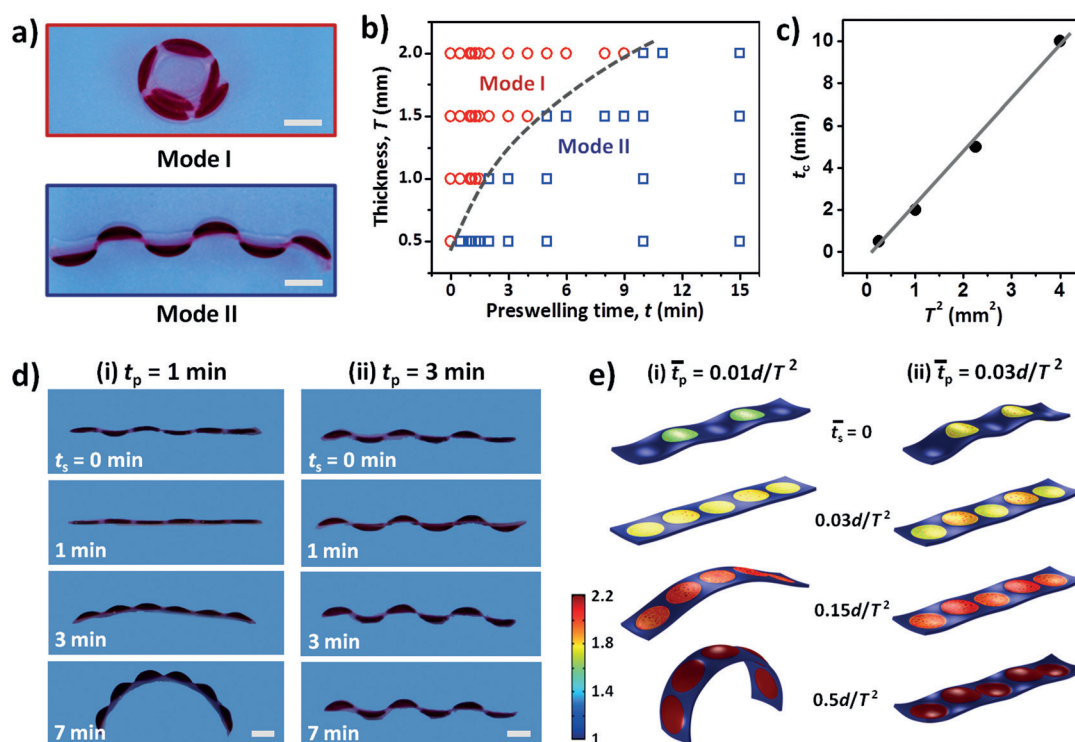
Figure 2. a) Photos of circular and sinusoidal shapes of the patterned gel strip formed without (mode I) and with the site-specific pre-swelling step (mode II). b),c) Effects of gel thickness and pre-swelling time on the final configurations of patterned gel strip (b) and the relationship between critical pre-swelling time, t_c, and gel thickness, T (c). d),e) Experimental (d) and computed (e) free-swelling-induced shape changing of the patterned gel after pre-swelling for a certain period of time. The pre-swelling time t_p and subsequent free-swelling time t_s were shown in (d), whereas dimensionless pre-swelling time $\bar{t}_p$ and free-swelling time $\bar{t}_s$ were used in (e). The color scale indicates the volumetric swelling ratio from the as-prepared state. Scale bar: 1 cm.

in through the unmasked side, the masked side swells less at a finite time. For the quasi 1D diffusion of the gel strip, T^2/d is the characteristic time for water to reach uniform distribution through the thickness, in which d is the self-diffusivity of water. Using a typical value of water diffusivity $d \approx 1 \times 10^{-9}$ m^2 s^{-1},[37,38] this corresponds to a characteristic time of $T^2/d \approx 10^3$ s for a 1 mm-thick gel. By changing the boundary conditions from non-permeable (masked) to given chemical potential (free-swelling) after a particular time in certain regions, numerical simulations of the kinetic swelling processes further confirmed the observations (Figure 2 e). The initial masked pre-swelling induces a through-thickness gradient of swelling ratio, resulting in the bending of disc gels into the masked sides. Shortly after removal of the mask, the deformation amplitudes decrease owing to the through-thickness redistribution of water and weakened through-thickness gradient. If the masked pre-swelling is insufficient, the buckling amplitude will drop to a neutral state in which the gel strip is almost flat, and subsequent unmasked swelling still leads to the energetically favorable buckling mode I. Although the characteristic time of the overall swelling agrees with that observed, the critical pre-swelling time $t_c \approx 0.01$–0.03 T^2/d is shorter than that found in the experiment. This is because of the lack of imperfection in computational models, so that switching between the bi-stable states (by overcoming an energy barrier) is more difficult. We should note that other factors such as the geometry of patterns and properties of gels

may also influence the energy barrier and thus the critical pre-swelling time.

Besides the above configurations, other morphing structures can also be easily programmed by using the same process but different masks. Since the buckling is induced by swelling mismatch between the high-swelling and non-swelling regions, the deformations of gels are fully reversible. The swelling mismatch can be diminished by de-swelling the P(AAm-co-AMPS) hydrogel in 0.15 M saline solution (Figure S1b). Subsequent swelling the gels in pure water will rebuild the mismatch and lead to macroscopic deformation again. Therefore, the pre-swelling step can be applied to guide the shape transformations of identical patterned hydrogel. In a similar way, masks with holes were placed on both sides of patterned gel flattened in saline solution, to guide the site-specific pre-swelling in pure water. As shown in Figure 3, various well-defined configurations were obtained on the same hydrogel sample.

This strategy can also be applied to hydrogel sheets patterned with a 2D array of high-swelling discs (Figure 4 a-(i)). Without the pre-swelling step, the patterned gel deformed into a roll (Figure 4 a(ii)), similar to the mode I deformation of gel strip shown in Figure 2 a. By using a pair of masks to direct the site-specific pre-swelling, other configurations, such as wavy and cruciform shapes, can be obtained (Figure 4 a(iii) and Figure 4 a(iv)). Large amplitude deformations can be realized in the patterned hydrogels with holes to
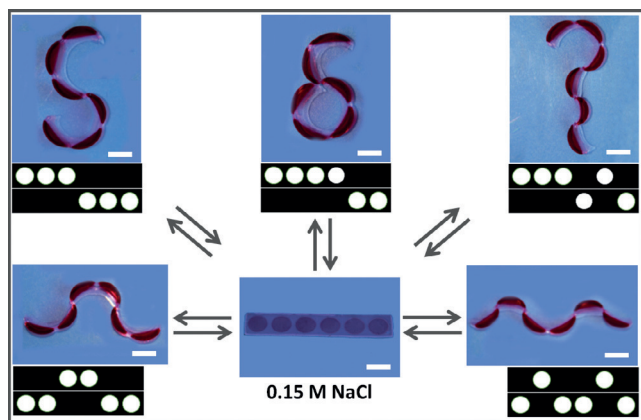
© 2017 Wiley-VCH Verlag GmbH & Co. KGaA, Weinheim

Figure 3. Morphing structures of identically patterned gel strips deformed in water with a pre-swelling step and flattened in 0.15 M saline solution. Pairs of masks with holes used to control the site-specific pre-swelling of the gel are shown under the photos. t_p was 10 min, and the gel achieved equilibrium state after 30 min. Scale bar: 1 cm.

under the same environmental condition. To our knowledge, such programmable, multiple 3D morphing structures of hydrogels have not been achieved in the previous studies.[9,22,30]

In conclusion, we have demonstrated a facile, versatile strategy to control the morphing structures of patterned hydrogels via a site-specific pre-swelling step. The selective pre-swelling of hydrogel induced a transient through-thickness gradient and therefore resulted in buckling in the desired direction. The programmed buckling of separate domains led to various morphing structures of the integrated patterned hydrogels. Since the deformations were induced by a stimuli-induced swelling mismatch, the deformed gel can be flattened under specific conditions, and shape transformations between programmed configurations can be realized by repeatedly using such site-specific pre-swelling steps. Although only a dome-shape was used in this work as the basic building block with self-locking capacity, other types of pattern, such
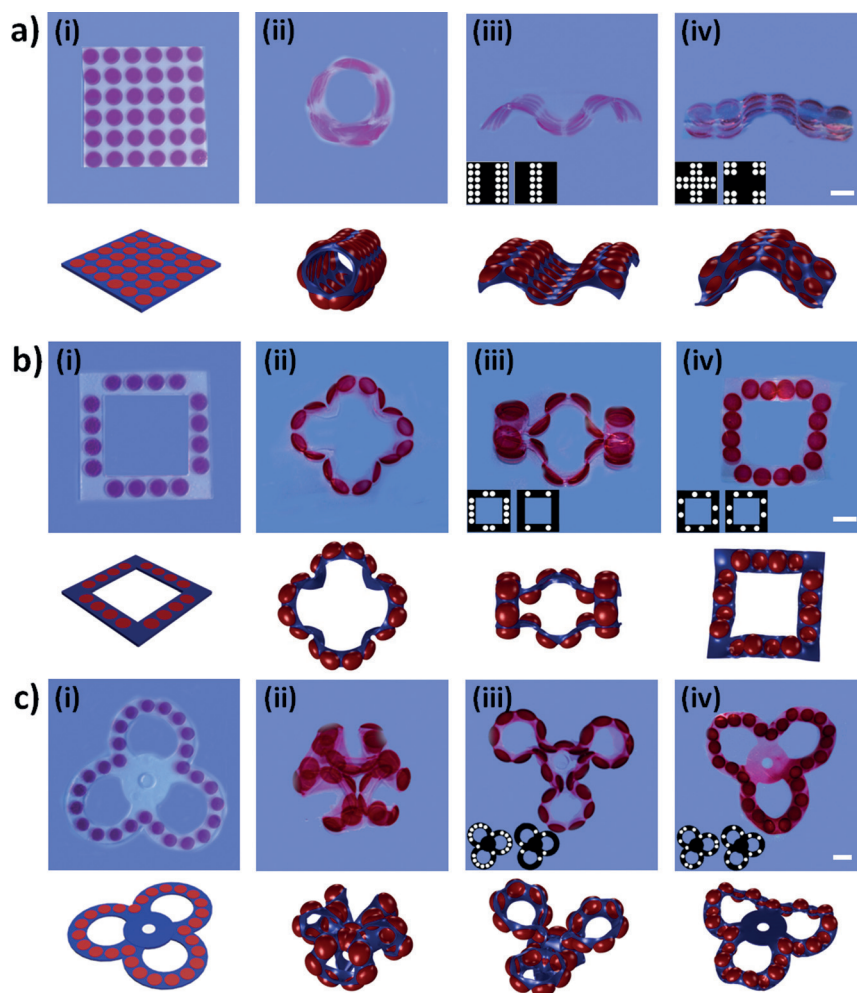
impart more deformation freedom, just like the kirigami structures.[39,40] For example, we prepared square or round loop patterned with high-swelling discs (Figures 4 b(i) and Figure 4 c(i)); the free-swelling (without the pre-swelling step) led to deformation of patterned gels into a four-pointed star and cauliflower-like configurations (Figures 4 b-(ii) and Figure 4 c(ii)), respectively, in which all domes buckled in the same direction yet constrained by the corner or central non-swelling gels. However, selectively pre-swelling led to localized buckling into opposite directions and thus the formation of desired configurations, such as the dumbbell-like and cloverleaf-like shapes (Figures 4 b(iii) and Figure 4 c(iii)). The buckling of neighboring domes can also be guided into different directions by pre-swelling approach, resulting in overall flat configurations (Figures 4 b(iv) and Figure 4 c(iv)). The modeled behaviors of patterned hydrogels consisted well with the experimental observations. We should note that the predefined overall pattern has a determining influence on the swelling-induced shape change of the hydrogel as a result of the geometric confinement. The localized deformations were distorted to some extent to accommodate the geometric continuity. Since the buckling direction of the separate domes can be encoded by the pre-swelling step with different masks, various morphing structures can be obtained in a single patterned hydrogel

Figure 4. Pre-swelling-directed shape morphing of patterned hydrogels. High-swelling gel discs were positioned in non-swelling gel in different ways (as-prepared state; the left column). After being swollen in water without (the second column) and with a pre-swelling step (the third and fourth columns), the patterned hydrogels deformed into distinct configurations. Insets: pair of masks used for site-specific pre-swelling. Computed configurations are also presented under the photos. The photos in each row correspond to the same patterned hydrogel. t_p was 10 min, and the gel achieved equilibrium state after 30 min. Scale bar: 1 cm.

as parallel stripes, can also be incorporated into the patterned hydrogels to enrich the programmable morphing structures. The in-plane gradient structures with controllable deformations mediated by a pre-swelling step can be combined with the through-thickness gradient structures of hydrogels to form more sophisticated configurations. The programming of multiple morphing structures should significantly expand the applications of active materials in biomedical devices and as soft actuators.

Conflict of interest

The authors declare no conflict of interest.

[1] Y. Liu, J. Genzer, M. D. Dickey, *Prog. Polym. Sci.* **2016**, *52*, 79.
[2] L. Ionov, *Adv. Funct. Mater.* **2013**, *23*, 4555.
[3] A. R. Studart, *Angew. Chem. Int. Ed.* **2015**, *54*, 3400; *Angew. Chem.* **2015**, *127*, 3463.
[4] S. Barbarino, O. Bilgen, R. M. Ajaj, M. I. Friswell, D. J. Inman, *J. Intell. Mater. Syst. Struct.* **2011**, *22*, 823.
[5] P. Fratzl, F. G. Barth, *Nature* **2009**, *462*, 442.
[6] S. Armon, E. Efrati, R. Kupferman, E. Sharon, *Science* **2011**, *333*, 1726.
[7] R. Elbaum, L. Zaltzman, I. Burgert, P. Fratzl, *Science* **2007**, *316*, 884.
[8] M. J. Harrington, K. Razghandi, F. Ditsch, L. Guiducci, M. Rueggeberg, J. W. C. Dunlop, P. Fratzl, C. Neinhuis, I. Burgert, *Nat. Commun.* **2011**, *2*, 337.
[9] R. Kempaiah, Z. Nie, *J. Mater. Chem. B* **2014**, *2*, 2357.
[10] S.-J. Jeon, A. W. Hauser, R. C. Hayward, *Acc. Chem. Res.* **2017**, *50*, 161.
[11] Z. Hu, X. Zhang, Y. Li, *Science* **1995**, *269*, 525.
[12] G. Stoychev, L. Guiducci, S. Turcaud, J. W. C. Dunlop, L. Ionov, *Adv. Mater.* **2016**, *26*, 7733.
[13] M. Jamal, A. M. Zarafshar, D. H. Gracias, *Nat. Commun.* **2011**, *2*, 527.
[14] J. Guo, T. Shroff, C. Yoon, J. Liu, J. C. Breger, D. H. Gracias, T. D. Nguyen, *Extrem. Mech. Lett.* **2017**, *16*, 6.
[15] R. M. Erb, J. S. Sander, R. Grisch, A. R. Studart, *Nat. Commun.* **2013**, *4*, 1712.
[16] E. Palleau, D. Morales, M. D. Dickey, O. D. Velev, *Nat. Commun.* **2013**, *4*, 2257.
[17] Q. Zhao, X. Yang, C. Ma, D. Chen, H. Bai, T. Li, W. Yang, T. Xie, *Mater. Horiz.* **2016**, *3*, 422.
[18] K.-U. Jeong, J.-H. Jang, D.-Y. Kim, C. Nah, J. H. Lee, M.-H. Lee, H.-J. Sun, C.-L. Wang, S. Z. D. Cheng, E. L. Thomas, *J. Mater. Chem.* **2011**, *21*, 6824.
[19] Y. Klein, E. Efrati, E. Sharon, *Science* **2007**, *315*, 1116.
[20] J. Kim, J. A. Hanna, M. Byun, C. D. Santangelo, R. C. Hayward, *Science* **2012**, *335*, 1201.
[21] Z. L. Wu, M. Moshe, J. Greener, H. Therien-Aubin, Z. Nie, E. Sharon, E. Kumacheva, *Nat. Commun.* **2013**, *4*, 1586.
[22] H. Thérien-Aubin, Z. L. Wu, Z. Nie, E. Kumacheva, *J. Am. Chem. Soc.* **2013**, *135*, 4834.
[23] M. Pezzulla, S. A. Shillig, P. Nardinocchi, D. P. Holmes, *Soft Matter* **2015**, *11*, 5812.
[24] Z. J. Wang, C. N. Zhu, W. Hong, Z. L. Wu, Q. Zheng, *J. Mater. Chem. B* **2016**, *4*, 7075.
[25] A. S. Gladman, E. A. Matsumoto, R. G. Nuzzo, L. Mahadevan, J. A. Lewis, *Nat. Mater.* **2016**, *15*, 413.
[26] J. H. Na, A. A. Evans, J. Bae, M. C. Chiappelli, C. D. Santangelo, R. J. Lang, C. T. Hull, R. C. Hayward, *Adv. Mater.* **2015**, *27*, 79.
[27] T. S. Shim, S.-H. Kim, C.-J. Heo, H. C. Jeon, S.-M. Yang, *Angew. Chem. Int. Ed.* **2012**, *51*, 1420; *Angew. Chem.* **2012**, *124*, 1449.
[28] J. S. Randhawa, T. G. Leong, N. Bassik, B. R. Benson, M. T. Jochmans, D. H. Gracias, *J. Am. Chem. Soc.* **2008**, *130*, 17238.
[29] C. Yoon, R. Xiao, J. Park, J. Cha, T. D. Nguyen, D. H. Gracias, *Smart Mater. Struct.* **2014**, *23*, 094008.
[30] A. Cangialosi, C. Yoon, J. Liu, Q. Huang, J. Guo, T. D. Nguyen, D. H. Gracias, R. Schulman, *Science* **2017**, *357*, 1126.
[31] X. Peng, Y. Li, Q. Zhang, C. Shang, Q.-W. Bai, H. Wang, *Adv. Funct. Mater.* **2016**, *26*, 4491.
[32] K. A. Seffen, *Scr. Mater.* **2006**, *55*, 411.
[33] D. P. Holmes, M. Roche, T. Sinha, H. A. Stone, *Soft Matter* **2011**, *7*, 5188.
[34] H. Lee, C. Xia, N. X. Fang, *Soft Matter* **2010**, *6*, 4342.
[35] W. Hong, X. Zhao, J. Zhou, Z. Suo, *J. Mech. Phys. Solids* **2008**, *56*, 1779.
[36] X. Wang, W. Hong, *Proc. R. Soc. London Ser. A* **2012**, *468*, 3824.
[37] H. Yasunaga, I. Ando, *Polym. Gels Networks* **1993**, *1*, 83.
[38] Y. Wu, S. Joseph, N. R. Aluru, *J. Phys. Chem. B* **2009**, *113*, 3512.
[39] N. Zheng, Z. Fang, W. Zou, Q. Zhao, T. Xie, *Angew. Chem. Int. Ed.* **2016**, *55*, 11421; *Angew. Chem.* **2016**, *128*, 11593.
[40] T. C. Shyu, P. F. Damasceno, P. M. Dodd, A. Lamoureux, L. Xu, M. Shlian, M. Shtein, S. C. Glotzer, N. A. Kotov, *Nat. Mater.* **2015**, *14*, 785.